

Limits on Surface Vicinality and Growth Rate due to Hollow Dislocation Cores on KDP {101}

J. J. De Yoreo, T. A. Land, and J. D. Lee

Department of Chemistry and Materials Science, Lawrence Livermore National Laboratory, Livermore, California 94550

(Received 6 January 1997)

Atomic-force microscopy measurements on KDP {101} faces are presented which show that the terrace width W on vicinal dislocation growth hillocks is nearly independent of supersaturation σ and Burgers vector b , in contradiction to simple Burton-Cabrera-Frank models. An analytical model taking into account the effect of dislocation cores on step rotation is presented which predicts a dependence of W on σ and b , in good agreement with the measurements. Using these results, we rescale macroscopic growth rate data onto a single Arrhenius curve, which gives a value of 0.33 eV for the activation energy of step motion. [S0031-9007(97)03298-5]

PACS numbers: 81.10.Aj, 61.16.Ch, 61.72.Lk, 68.35.Bs

Growth of smooth surfaces during epitaxy is a central problem in materials science. Application of conditions which favor layer-by-layer growth rather than multilayer growth is generally recognized to produce smoother surfaces and more abrupt interfaces [1,2]. In particular, growth in a step-flow model ensures that incoming atoms become attached at existing kink sites on a regular array of steps, producing well-defined vicinality.

Step-flow growth is most easily produced in a near-equilibrium regimes, where the morphology is likely to be controlled more by equilibrium thermodynamic considerations [3] than by the kinetic factors often associated with nucleation of new islands [4]. During growth of inorganic crystals from low temperature aqueous solutions, the range of supersaturation which is typically accessible leads to critical island sizes consisting of $\sim 10^3$ molecules. Thus, unless great care is taken to ensure that the initial seed crystal is dislocation free, growth occurs almost exclusively by step flow on vicinal hillocks formed by dislocations. Consequently, investigations of surface morphological evolution in such systems can provide important insights into the controls on surface roughness and growth rate during epitaxial growth in a step-flow regime.

Previously [5–7], we showed that atomic-force microscopy (AFM) could be used to investigate the morphology and dislocation structure of growth hillocks on solution grown crystals both *ex situ* [5] and *in situ* [6,7]. In this Letter, we use AFM measurements on the {101} face of KH_2PO_4 (KDP) grown from aqueous solution to investigate the dependence of surface vicinality on supersaturation and dislocation structure. We find that, over the range of supersaturation $0.03 \leq \sigma \leq 0.31$, terrace width is nearly independent of both supersaturation and dislocation structure, in contradiction to the predictions of the simple model of Burton, Cabrera, and Frank (BCF) [3]. We show that an analytical model that takes into account the effect of hollow dislocation cores on the period of step rotation predicts a dependence of terrace width on supersaturation and Burgers vector which is in good agreement with the measured slopes. These results are used to explain the reproducible character of macroscopic growth

rates and to rescale data on growth rate as a function of temperature and supersaturation onto a single curve. This curve has an Arrhenius form and gives a value of 0.33 eV for the activation energy of step motion.

Two types of experiments were performed: Samples were measured both *in situ* [6–8] at low supersaturations ($\sigma < 0.01$) under conditions of flowing solution and *ex situ* [5,8] on samples grown in the range of $0.03 \leq \sigma \leq 0.25$ and imaged in air. In both cases, atomic-force microscopy was done in contact mode with standard SiN cantilevers having a nominal force constant of 0.1 nN/nm. The supersaturation σ was calculated from $\sigma \equiv \Delta\mu/kT = \ln(C/C_o)$, where $\Delta\mu$ is the change in chemical potential upon crystallization, k is Boltzmann's constant, T is the absolute temperature, and C and C_o are the actual and equilibrium molarities. Experimental details are presented elsewhere [8].

Figure 1(a) is a schematic of a KDP crystal along with the hillock geometry on both the {100} and {101} faces. Figure 1(b) shows an *in situ* AFM image near the top of a

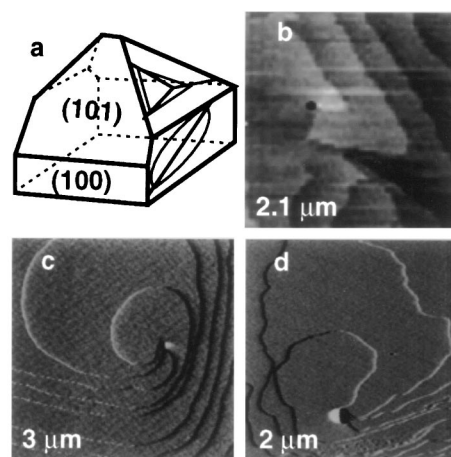


FIG. 1. (a) Schematic showing geometry of growth hillocks on KDP. (b) $2.1 \mu\text{m}$ *in situ* AFM image near top of growth hillock on KDP {101} showing the presence of hollow core and step structure near the core. (c) $3.0 \mu\text{m}$ and (d) $4.0 \mu\text{m}$ images of typical hillocks with $b_{\perp} = 3h$ and $4h$, respectively.

typical dislocation hillock on the $\{101\}$ face for which the component of the Burgers vector perpendicular to the surface, $b_{\perp} = mh$, is two unit step heights, $2h$. Figures 1(c) and 1(d) are *ex situ* images of hillocks formed by dislocation sources for which b_{\perp} is $3h$ and $4h$, respectively. As the *in situ* image shows, hillocks on KDP $\{101\}$ consist of straight-line steps emerging from a hollow dislocation core and oriented along the three step directions on the $\{101\}$ face. (The rounded corners apparent in the *ex situ* images result from postgrowth annealing [9].) The relative slopes of each of the three vicinal sectors on these hillocks are determined by kinetic factors [10]. In accordance with their relative slopes, we refer to the three sectors as the shallow, medium, and steep sectors, respectively.

Figure 2 shows the dependence of hillock slope p on supersaturation for each of the three sectors at values of σ between 0.03 and 0.25. (Little data is shown for the steepest sector because, over most of the experimental range, the slope was too great to allow for accurate measurements.) The data show that, regardless of the value of b_{\perp} , the hillock slope rises abruptly until $\sigma \sim 0.05$, beyond which it rises slowly and appears to approach a limiting value.

In their classical paper on the growth of single crystals, Burton, Cabrera, and Frank [3] presented the basic rela-

tionships between the structure of a dislocation source and the vicinity of the resultant growth hillock. In this simple model, the morphology of the crystal surface is determined solely by the two experimental parameters: the supersaturation and the temperature, and two materials parameters; the free energy of step edge and the height of an elementary step, along with the net Burgers vector and lateral extent of the dislocation source. The BCF model predicts that the hillock slope p for an isotropic spiral should be given by [3,11]

$$p = \frac{mh}{19r_c + 2L}, \quad (1a)$$

$$r_c = \frac{\Omega\alpha}{kT\sigma}, \quad (1b)$$

where mh is the number of unit steps in b_{\perp} , $2L$ is the length of the perimeter at the surface surrounding the group of dislocations which create the hillock, r_c is the critical radius, Ω is the inverse of the number density of molecules in the solid, and α is the free energy of the step edge per unit step length per unit step height. In the case of an anisotropic triangular hillock, Eq. (3) can be approximated by [10]

$$p_i = \frac{0.547mh}{\beta_i(\ell_c B + L^*)}, \quad (2a)$$

$$\ell_c = 2\sqrt{3}r_c, \quad B = \sum_{i=1}^3 \frac{1}{\beta_i}, \quad L^* = \sum_{i=1}^3 \frac{L_i}{\beta_i}, \quad (2b)$$

where ℓ_c is the critical length of a step segment, L_i is the length of the i th side of a triangle enclosing the dislocation bunch, and β_i/β_j is given by the inverse of the ratio of the slopes of the i th and j th sectors of the hillock. The values of the parameters in Eq. (2) are known and are given in Table I. When $L = 0$, the dependence of hillock slope on supersaturation predicted by the BCF model is linear in σ and, for $m = 1$, is given by the dashed lines in Fig. 2. For larger values of m , the slopes of the predicted curves should scale linearly with m . In contrast to these predictions, the measured slope is highly nonlinear in σ and shows almost no dependence on the size of the Burgers vector. We will now show that the reason for this discrepancy is that the simple model ignores the effect of the dislocation cores.

Frank [14] and Cabrera and Levine [11] showed that, in general, the strain field associated with a dislocation should produce a hollow core provided that the ratio of the elastic energy to the free energy of the step edge is sufficiently large. Hollow dislocation cores have been observed in a number of materials including epitaxially grown films of GaN [15]. Previously, we reported AFM observations of dislocation cores in KDP [5]. These cores are also seen in Fig. 1. As shown by van der Hoek *et al.* [16], the radius of the hollow core r_{hc} is \leq the Frank radius r_F which, for an isotropic solid, is given by [14]

$$r_F = \frac{Gb^2}{8\pi^2\alpha_F}, \quad (3)$$

where $G = (c_{11} - c_{12})/2$ is the modulus of rigidity, α_F is the free energy per unit length per unit step height

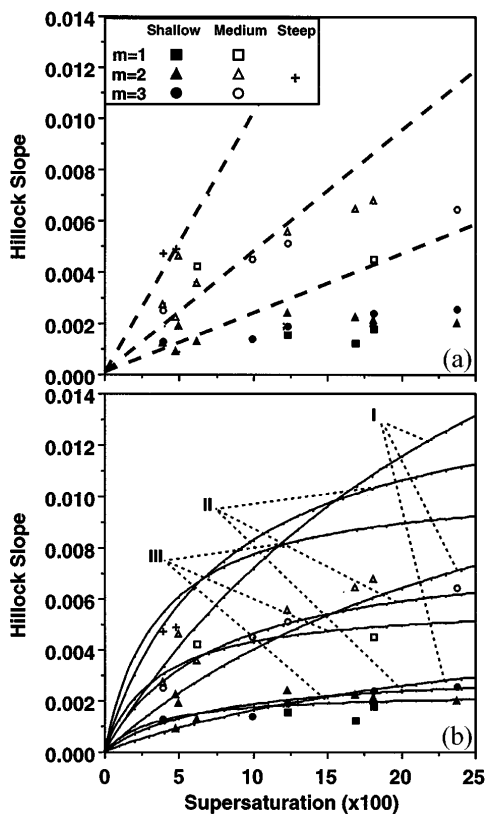


FIG. 2. Measured hillock slope (data points) versus supersaturation along with (a) curves predicted by BCF model for $m = 1$ (dashed lines), and (b) those predicted by Eq. (7) (solid lines) for I: $r_0 = 3$ nm at $m = 1$, II: $r_0 = 12$ nm at $m = 2$, and III: $r_0 = 25$ nm at $m = 3$, where r_0 is the radius of the hollow core.

TABLE I. Experimental values of parameters used in evaluating Eqs. (2), (3), (7), and (8).

Ω (cm ³ /molecule)	h (10 ⁻⁷ cm)	α [12] (erg cm ⁻²)	G [13] (erg cm ⁻³)	β_3/β_2	β_2/β_1	ϕ_1	ϕ_2	ϕ_3
9.68×10^{-23}	0.5086	20	3.844×10^{11}	2.5	1.8	159°	119°	82°

inside the core, and b is the magnitude of the Burgers vector. As discussed elsewhere [5], for the growth conditions in this study, r_{hc} is about one-half of r_F . Figure 3 shows that both the magnitude and the dependence of the measured core radii on m are consistent with Eq. (3).

When a dislocation source generates a hollow core of radius r_{hc} , the step must spiral around this core in order for the surface to advance. Thus, as a result of core formation, even when the dislocation source is simple (that is, all steps emerge from a single source), we should expect that $2L$ is nonzero and of order $2\pi r_{hc}$. To quantitatively analyze the experimental results, we now calculate the slope of an anisotropic, triangular hillock with a dislocation core following the scheme of Vekilov *et al.* [10] and based on the geometry shown in Fig. 4. A triangular spiral makes on full rotation about a core of radius r_0 , in time τ given by

$$\tau = \frac{L_1 + \ell_c}{v_2} + \frac{L_2 + \ell_c}{v_3} + \frac{L_3 + \ell_c}{v_1}, \quad (4)$$

where L_i is the length of the chord of the dislocation core along the step direction in the i th sector, and v_i is the step velocity in the i th sector. The slope of the i th sector is given by

$$p_i = \frac{mh}{v_i\tau} = \frac{mh\omega}{v_i \sum_{j=1}^3 \frac{L_j + \ell_c}{v_{j+1}}}, \quad (5)$$

where $v_4 = v_1$ and ω , which approximates the influence of the Gibbs-Thomson effect, equals 0.547 for a triangular step [17]. We now assume that step speed is linear in concentration such that the step speed far from the dislocation source v_i is given by

$$v_i = \Omega\beta_i(C - C_o), \quad (6)$$

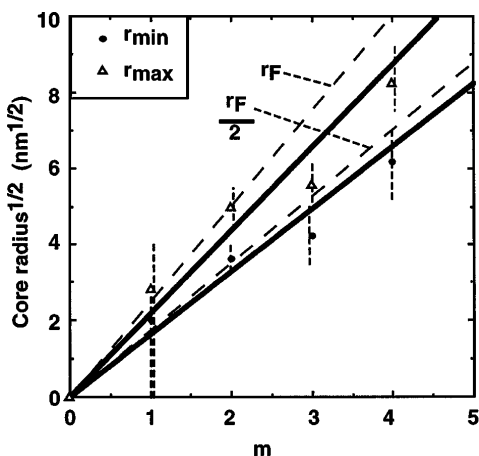


FIG. 3. Dependence of core radii on Burgers vector. r_{\min} and r_{\max} are the measured core radii at half depth and at the surface, respectively. Dashed lines for r_F and $r_F/2$ were calculated from Eq. (5) assuming $K = 1$ and $\alpha_F = \alpha$.

where C and C_o are the actual and equilibrium concentrations. This has been shown to hold for a number of systems [10,12,18], including KDP [12], and has a theoretical basis [19,20]. From the geometry of the hillock we see that $L_j \cong 2r_0 \sin(\phi_j/2)$, where r_0 is the radius of the channel and ϕ_i is defined in Fig. 4. Combining Eqs. (4)–(6) gives

$$p_i = \frac{mh\omega}{\beta_i(2\sqrt{3}r_cB + r_0\Phi)}, \quad (7a)$$

$$B = \sum_{j=1}^3 \frac{1}{\beta_j}, \quad \Phi = \sum_{j=1}^3 \frac{2 \sin(\phi_{j+1}/2)}{\beta_j}. \quad (7b)$$

The values of β_i/β_j and ϕ_i are given in Table I for our measurements on KDP {101}.

The solid curves in Fig. 2 give the predicted curves for $r_0 = 3$ nm at $m = 1$, $r_0 = 12$ nm at $m = 2$, and $r_0 = 25$ nm at $m = 3$ which are consistent with the measured core radii in Fig. 3. The predicted curves are in good agreement with the measured dependence of p on σ . From these results we conclude that, due to the presence of the hollow cores above approximately $\sigma = 0.05$, the hillock slopes are weakly dependent on σ and nearly independent of b_{\perp} .

The normal growth rate R of a crystal face growing on a dislocation hillock is given by $R = pv$. Using Eq. (6), we have

$$R = p_i\Omega\beta_i(C - C_o). \quad (8)$$

Because the growth of macroscopic KDP crystals begins with the nondeterministic process of seed regeneration [12,21], the dislocation structure of the leading hillocks will vary greatly from one growth run to another. If the hillock slope was strongly dependent on the structure of the dislocation source as predicted by the simple BCF model, then the growth rate would also vary greatly from run to run. Zaitseva *et al.* [21] reported the dependence of σ on T at a constant growth rate along the {001}

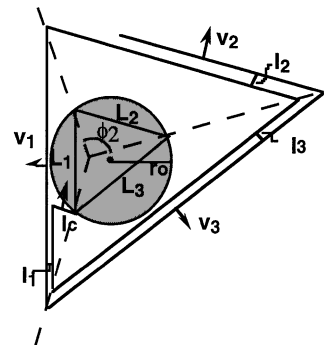


FIG. 4. Model hillock and core geometry used in deriving Eq. (7).

direction ($R_{\{001\}} = \sqrt{2}R_{\{101\}}$). The authors found that these growth rates were reproducible from run-to-run. From the experimental results and analysis presented in this paper, we now understand that, because v is a function only of T and $C - C_o$, and p is weakly dependent on dislocation structure, we should expect R to be well defined only by T and σ . We have taken the growth rate data of Zaitseva *et al.* [21] (shown in the inset of Fig. 5) and calculated the slope at each supersaturation from a fit to our data on $p(\sigma)$ in Fig. 3. As Fig. 5 shows, when R is normalized by $p(C - C_o)$ all of the growth rate data fall onto a single curve which follows an Arrhenius relationship. The slope of this curve gives an activation energy for step motion of 0.33 eV. Because the ratio of the slopes of the shallow and medium sectors is a constant over the range of experimental range, the same result is obtained for both sectors.

Growth of crystals from solution is a multistage process involving adsorption, diffusion, and incorporation at the step edge. Consequently, the measured activation energy only gives the effective energy barrier between the initial solvated state and the final state at the step edge. However, because the same activation energy is obtained for both sectors, the differences in step kinetics which are responsible for the different slopes on these sectors must arise from differences in either jump distances during diffusion or attempt frequencies during incorporation.

In the BCF model, the step-edge free energy is the fundamental material parameter controlling the surface morphology. It determines ℓ_c (or r_c) and, therefore, determines both how tightly a spiral will wind and when 2D nucleation will begin. However, as Eqs. (3) and (7) show, when vicinality is controlled by the dislocation cores, the elastic constants of the material exert as much control over surface vicinality as does the step-edge free energy. In addition, because the magnitude of the slope reaches a limiting value with increasing σ , the value of

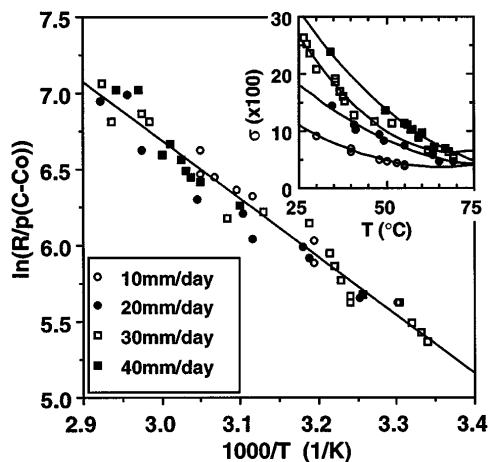


FIG. 5. Dependence of $\ln\{R/[p(C - C_o)]\}$ on T derived from measurements (shown in the inset) of σ required to maintain constant $R_{\{101\}}$ during KDP growth by temperature drop [21].

σ at which 2D nucleation begins will be reduced, simply because diffusing adatoms are farther from a step edge [1]. The conclusion of this study is that, on KDP $\{101\}$ surfaces, the consequences of this effect are (1) for $0.05 \leq \sigma \leq 0.25$, the terrace widths on vicinal growth hillocks formed by dislocations are controlled by the size of the hollow cores associated with the dislocation source, and (2) the growth rate is determined solely by the values of T and σ , and is nearly independent of dislocation structure.

This work was performed under the auspices of the U.S. Department of Energy by Lawrence Livermore National Laboratory under Contract No. W-7405-ENG-48.

- [1] J. Tersoff, A. W. Denier van der Gon, and R. M. Tromp, *Phys. Rev. Lett.* **72**, 266 (1994).
- [2] J. E. Van Nostrand, S. J. Chey, M.-A. Hasan, D. G. Cahill, and J. E. Greene, *Phys. Rev. Lett.* **74**, 1127 (1995).
- [3] W. K. Burton, N. Cabrera, and F. C. Frank, *R. Soc. London Philos. Trans.* **A243**, 299 (1951).
- [4] J. G. Amar and F. Family, *Phys. Rev. Lett.* **74**, 2066 (1995).
- [5] J. J. De Yoreo, T. A. Land, and B. J. Dair, *Phys. Rev. Lett.* **73**, 838 (1994).
- [6] T. A. Land, A. J. Malkin, Yu. G. Kuznetsov, J. J. De Yoreo, and A. McPherson, *Phys. Rev. Lett.* **75**, 2774 (1995).
- [7] A. J. Malkin, T. A. Land, Yu. G. Kuznetsov, A. McPherson, and J. J. De Yoreo, *Phys. Rev. Lett.* **75**, 2778 (1995).
- [8] J. J. De Yoreo, T. A. Land, L. N. Rashkovich, T. A. Onischenko, J. D. Lee, O. V. Monovskii, and N. P. Zaitseva, *J. Cryst. Growth* (to be published).
- [9] T. A. Land, J. J. De Yoreo, and J. D. Lee, *Surf. Sci. A* (to be published).
- [10] P. G. Vekilov, Yu. G. Kuznetsov, and A. A. Chernov, *J. Cryst. Growth* **121**, 643 (1992).
- [11] N. Cabrera and M. M. Levine, *Philos. Mag.* **1**, 450 (1956).
- [12] L. N. Rashkovich, *KDP Family of Single Crystals* (Adam-Hilger, New York, 1991).
- [13] *Landolt-Bornstein Tables of Numerical Data and Functional Relationships in Science and Technology*, edited by K.-H. Hellwege and A. M. Hellwege (Springer, New York, 1979), Group III, Vol. 11.
- [14] F. C. Frank, *Acta Crystallogr.* **4**, 497 (1951).
- [15] W. Qian, G. S. Rohrer, M. Skowronski, K. Doverspike, L. B. Rowland, and D. K. Gaskill, *Appl. Phys. Lett.* **67**, 2284 (1995).
- [16] B. Van der Hoek, J. P. Van der Eerden, and P. Bennema, *J. Cryst. Growth* **56**, 621 (1982).
- [17] E. Budevski, G. Staikov, and V. Bostanov, *J. Cryst. Growth* **29**, 316 (1975).
- [18] A. J. Malkin, Yu. G. Kuznetsov, W. Glantz, and A. McPherson, *J. Phys. Chem.* (to be published).
- [19] A. A. Chernov, *Sov. Phys.* **4**, 116 (1961).
- [20] G. H. Gilmer, R. Ghez, and N. Cabrera, *J. Cryst. Growth* **8**, 79 (1971).
- [21] N. P. Zaitseva, I. L. Smolsky, and L. N. Rashkovich, *Kristallografiya* **36**, 198 (1991) [*Sov. Phys. Crystallogr.* **36**, 113 (1991)].